Diastereomeric Crowding Effects in the Competitive DNA Intercalation of Ru(phenanthroline)2dipyridophenazine2+ Enantiomers

Inorganic Chemistry
Cite This: Inorg. Chem. 2019, 58, 9452−9459
Article
pubs.acs.org/IC

Diastereomeric Crowding Effects in the Competitive DNA Intercalation of Ru(phenanthroline)$_2$dipyridophenazine^{2+} Enantiomers

Anna K. F. Mårtensson,[†] Maria Abrahamsson,[†] Eimer M. Tuite,[‡] and Per Lincoln*[,†]

[†]Department of Chemistry and Chemical Engineering, Chalmers University of Technology, Kemigården 4, SE-412 96 Gothenburg, Sweden

[‡]School of Chemistry, Newcastle University, Bedson Building, Newcastle upon Tyne NE1 7RU, U.K.

Supporting Information

ABSTRACT: The biexponential excited-state emission decay characteristic of DNA intercalated tris-bidentate dppz-based ruthenium complexes of the general form Ru(L)$_2$dppz^{2+} has previously been explained by a binding model with two distinct geometry orientations of the bound ligands, with a distinct lifetime associated with each orientation. However, it has been found that upon DNA binding of Ru(phen)$_2$dppz^{2+} the fractions of short and long lifetimes are strongly dependent on environmental factors such as salt concentration and, in particular, temperature. Analyzing isothermal titration calorimetry for competitive binding of Ru(phen)$_2$dppz^{2+} enantiomers to poly(dAdT)$_2$, we find that a consistent binding model must assume that the short and long lifetimes states of intercalated complexes are in equilibrium and that this equilibrium is altered when neighboring bound ligands affect each other. The degree of intercomplex binding is found to be a subtle manifestation of several attractive and repulsive factors that are highly likely to directly reflect the strong diastereomeric difference in the binding enthalpy and entropy values. In addition, as the titration progresses and the binding sites on the DNA lattice become increasingly occupied, a general resistance for the saturation of the binding sites is observed, suggesting diastereomeric crowding of the neighboring bound ligands.

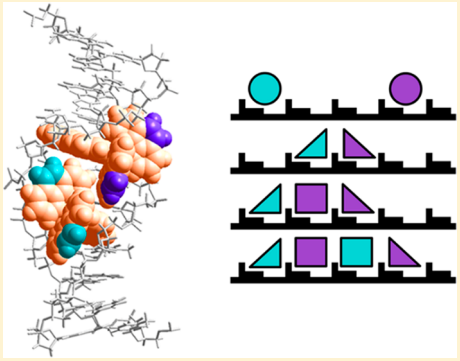

INTRODUCTION

The discovery of the "light-switch" complex, Ru(bpy)$_2$dppz^{2+} (Ru-bpy; bpy = 2,2′-bipyridine; dppz = dipyrido[3,2-*a*:2′,3′-*c*]phenazine), by Barton and Sauvage almost 30 years ago was soon followed by the discovery of Ru(phen)$_2$dppz^{2+} (Ru-phen; phen = 1,10-phenanthroline) and initiated the synthesis of many variations of DNA-based ruthenium-centered tris-bidentate complexes.[1−3] Having interesting photophysical properties together with a strong binding affinity for DNA and a slight selectivity for A-T base pairs has made such DNA intercalative complexes attractive candidates for new pharmacological therapeutics and biosensors.[4,5] The luminescence of these complexes, attributed to a dppz-localized ^{3}MLCT excited state,[6−10] is effectively quenched in hydroxylic solvents; to be completely extinguished, the 9- and 14-nitrogens of the extended (phenazine) part of the dppz ring system are required to be H-bonded in the excited state.[11] However, when the phenazine nitrogens are shielded from forming H-bonds with the water molecules in a hydrophobic environment, such as between the DNA base pairs, their luminescence is turned on. Even more interestingly, when bound to DNA, complexes of the general form Ru(L)$_2$dppz^{2+} (L = ancillary polypyridyl ligand) exhibit almost invariably a biexponential excited-state emission decay.[1,12−14]

Octahedral tris-bidentate ruthenium complexes of the general form Ru(L)$_2$dppz^{2+} are chiral and adopt a structure much like a three-winged propeller, which can have a right-handed (Δ) or a left-handed (Λ) configuration (Scheme 1).

Scheme 1. Structures of Λ-Ru(phen)$_2$dppz^{2+} (left) and Δ-Ru(phen)$_2$dppz^{2+} (right)

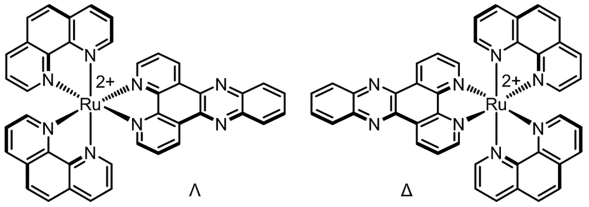

DNA is itself a chiral molecule, being a right-handed helical structure in its common B-form. Not surprisingly, diastereomeric effects are observed when enantiopure Ru-bpy or Ru-phen is intercalated to DNA, where both spectroscopic and calorimetric studies report a generally stronger binding affinity for the Δ enantiomer than for the Λ enantiomer.[14−20] The two

Received: May 3, 2019
Published: June 24, 2019

emission lifetimes observed for both Ru-bpy and Ru-phen have previously been assigned to two distinct binding geometries, where the shorter lifetime is attributed to complexes centered in the intercalation pocket and the longer lifetime is from a more canted intercalation geometry (Figure 1).[17,21,22] This has further been supported by recent X-ray crystallography studies, reporting differently angled intercalation geometries for intercalation from the minor groove for Λ-Ru-phen.[23,24]

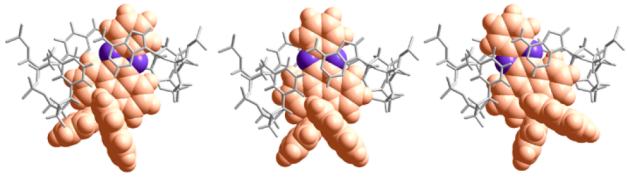

Figure 1. Schematic illustration of the proposed binding geometries of the canted intercalation geometry (left and right) and the centered intercalation geometry (middle) of Δ-Ru-phen viewed from above the DNA helix axis. The 9- and 14-nitrogens on the extended part of the dppz moiety are colored purple.

Both photophysical data and calorimetric data have previously revealed the DNA binding characteristics of the Λ enantiomers of Ru-bpy and Ru-phen to be very similar to each other, in terms of the relative contributions from the two emitting species, excited-state lifetimes, and very similar calorimetric titration isotherms.[17,21] In contrast, the binding characteristics of the Δ enantiomers are much more different in appearance, indicating the strong influence of the 1,10-phenanthroline B ring, which is missing in 2,2′-bipyridine. The DNA molecule can be considered as a long polymer of binding sites that, when occupied by bulky structures such as Ru-bpy and Ru-phen, overlap each other. Therefore, in any binding model to give a satisfactory global fit, cooperativity effects must be included, meaning that bound neighboring ligands may affect the binding geometry orientations of each other.[17,20,25] In our first global analysis of isothermal titration calorimetry (ITC) and luminescence data for Ru-dppz complexes, the differences between the Δ enantiomers were suggested to originate from a preference for doublet formation, canted away from each other, already at low binding densities of Δ-Ru-phen, whereas Δ-Ru-bpy was suggested to prefer a centered intercalation of single complexes at the same, low binding densities.[17]

Initially, we modeled the DNA strand as a homopolymer of identical intercalation pockets using a generalized McGhee–von Hippel[26] binding isotherm algorithm.[17,25] While this method[27] accounted for binding site interactions, it was still a complicated algorithm with limited efficiency that never gained widespread use. Recently, we have developed a much simplified algorithm that is very general and can be utilized for modeling binding of a ligand to any type of linear biopolymer.[20] We demonstrated the practical usage of this algorithm by a series of competitive ITC experiments in which enantiopure Ru-bpy was titrated into poly(dAdT)$_2$ (AT-DNA) already saturated by the opposite enantiomer.

While for Ru-bpy it is possible to fit calorimetric data to a simpler binding model with only one assumed binding geometry, the enthalpic changes for Ru-phen interacting with DNA are more prominent and might require a more complicated binding model. Although the earlier model for Ru-phen with two distinct binding geometries accounts for the two emission lifetimes, it does not satisfactorily explain why the fractions of short and long lifetimes appear to be dependent on temperature and salt concentration in more recent results.[22] In this study, we seek to evaluate the earlier binding model for Ru-phen in a competitive setting as we did previously for Ru-bpy. Our aim is to find an improved binding model that also accounts for the more recent extensive photophysical research performed on the ligand–DNA characterization of Ru-phen, using our newly developed simplified general algorithm. Rather than two distinct binding geometries, our improved binding model proposes that all intercalated complexes are regarded to be in equilibrium between a short and long lifetime state, and this equilibrium is affected by the intercomplex cooperativity between neighboring ligands.

EXPERIMENTAL SECTION

Materials and Sample Preparation. Enantiopure Δ-[Ru(phen)$_2$dppz]Cl$_2$ and Λ-[Ru(phen)$_2$dppz]Cl$_2$ were prepared as previously reported.[14] Other chemicals were purchased from Sigma-Aldrich and used without purification.

All experiments were performed in an aqueous buffer solution (pH 7.0) containing 150 mM NaCl and 1 mM cacodylate (dimethylarsinic acid sodium salt). A stock solution of poly(dAdT)$_2$ (AT-DNA) (∼5 mM nucleotides) was prepared by dissolving the sodium salt (Sigma-Aldrich) in a buffer solution. For ITC measurements, the DNA solution was dialyzed against pure buffer for at least 48 h at 8 °C. The dialysis membrane used had a molecular weight cutoff of 3.5–5 kDa (Spectra-Por Float-A-Lyzer G2, Sigma-Aldrich). Stock solutions of the ruthenium complexes (∼1 mM) were prepared by dissolving the chloride salts in a buffer solution. Concentrations were determined spectrophotometrically using the following extinction coefficients: ε_{262} = 6600 M^{-1} cm^{-1} for poly(dAdT)$_2$; ε_{440} = 20000 M^{-1} cm^{-1} for Ru(phen)$_2$dppz^{2+}. Ruthenium complex solutions of appropriate concentrations were prepared by dilution of the stock solutions in the dialysate.

Absorption spectra were measured on a Varian Cary 4000 UV/vis spectrophotometer (Agilent Technologies) (path length of 1 cm).

Isothermal Titration Calorimetry. Isothermal titration calorimetry (ITC) has many advantages when studying the binding interactions between biomolecules and is often termed the "gold standard" for quantitative measurements of ligand–macromolecule associations. It is also the only method capable of direct thermodynamic measurement of all of the energetics associated with the binding interaction process, enabling a full thermodynamic characterization (stoichiometry, association constant, and enthalpy and entropy of binding).[28−30] It is a high-precision tool in which the heat produced or absorbed upon addition of the complex to a DNA solution enables direct assessment of the binding enthalpy by integrating the power required to maintain the reference and sample cells at the same temperature. The experimental raw data consist of a series of heat flow peaks, and each peak corresponds to one injection of complex. These heat flow peaks are integrated with respect to time, which give the total heat exchanged per mole of injectant plotted against the [Ru]/[base pairs] ratio.

Calorimetric data were obtained using a MicroCal iTC200 isothermal titration calorimeter (Malvern Instruments) controlled by Origin 7.0 software. The ITC profiles of the Δ and Λ enantiomers of Ru-phen were obtained by a single injection of 1 μL followed by 19 sequential titrations in 2 μL aliquot injections of a complex from a syringe stock solution (∼550 μM) into the sample cell (206 μL) loaded with AT-DNA in a 150 mM NaCl aqueous solution (∼408 μM nucleotides). We chose to use AT-DNA for the ligand–DNA interaction to avoid any effects from DNA heterogeneity and the possible quenching of the MLCT excited state by electron transfer from guanine.[21]

This was subsequently followed by an additional 20 sequential injections (single injection of 1 μL followed by 19 injections of 2 μL aliquots) of the opposite enantiomer into the sample cell now loaded

DOI: 10.1021/acs.inorgchem.9b01298
Inorg. Chem. 2019, 58, 9452−9459

with AT-DNA saturated by the first complex. The injection spacing was 180 s; the syringe rotation was 1000 rpm, and there was an initial delay of 120 s prior to the first injection. Negligible heat arose from DNA dilution. The raw ITC data peaks were automatically integrated using the Origin 7.0 software. For the improved accuracy of integration, the integration range for the spacing between each peak was narrowed, thus reducing the background noise from the baseline.

Binding Models. A ligand bound to a homogeneous one-dimensional lattice of binding sites can be in three distinct environments: either isolated, i.e., without any ligand neighbors, with one ligand neighbor on one side and one empty binding site on the other (end binding), or with neighbors on both sides (interior binding). In the study presented here, we have used two models: model A, in which the ligand−ligand interaction energy is assumed to be additive and independent of the environment, and model B, in which the ligand−ligand interaction energies may be taken to be different for ligands at ends or in the interior of a sequence of consecutively bound ligands.

In model B, this is modeled by four different elementary units (two unsymmetrical units *a* and *b*, occurring only to the left and right, respectively, of a ligand neighbor, and two symmetrical units, *c*, occurring only in the interior of ligand sequences, and *d*, which only occur isolated). In the earlier model (denoted model C) proposed by Andersson et al.,[17] there is only one symmetrical elementary unit *c* that can occur both isolated and in the interior of ligand sequences. In addition, *c* may also be an end unit when bound next to either *a* or *b*. In model B, this arrangement is not allowed but the end unit must be an unsymmetrical unit. Model C and model B are illustrated in Figure 2. For the simultaneous binding to a lattice of two different ligands 1 and 2, the cooperative factor matrix **Y** then becomes

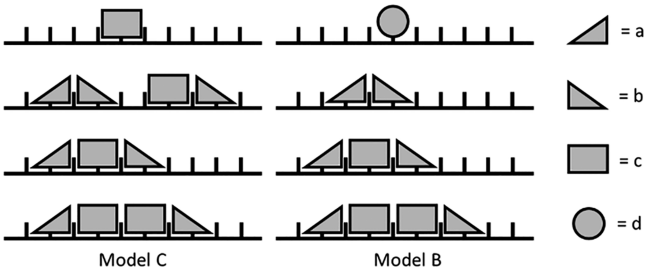

Figure 2. Schematic illustration comparing the old lattice model C (left) with the proposed lattice model B (right) showing the four different elementary units and their allowed ligand−DNA interactions.

$$\begin{bmatrix} 1 & 1 & 0 & 0 & 1 & 1 & 0 & 0 & 1 \\ 0 & 0 & Ya1b1 & Ya1c1 & 0 & 0 & Ya1b2 & Ya1c2 & 0 \\ 1 & 0 & 0 & 0 & 0 & 0 & 0 & 0 & 0 \\ 0 & 0 & Yc1b1 & Yc1c1 & 0 & 0 & Yc1b2 & Yc1c2 & 0 \\ 1 & 0 & 0 & 0 & 0 & 0 & 0 & 0 & 0 \\ 0 & 0 & Ya2b1 & Ya2c1 & 0 & 0 & Ya2b2 & Ya2c2 & 0 \\ 1 & 0 & 0 & 0 & 0 & 0 & 0 & 0 & 0 \\ 0 & 0 & Yc2b1 & Yc2c1 & 0 & 0 & Yc2b2 & Yc2c2 & 0 \\ 1 & 0 & 0 & 0 & 0 & 0 & 0 & 0 & 0 \end{bmatrix} \quad (1)$$

The lattice with bound ligands is symmetrical; thus, $Ya1c1 = Yc1b1$, $Ya2c2 = Yc2b2$, $Ya1b2 = Ya2b1$, $Ya1c2 = Yc2b1$, $Ya2c1 = Yc1b2$, and $Yc1c2 = Yc2c1$, but in general, $Ya1c2 \neq Ya2c1$.

If all cooperativity factors involving a particular pair of ligands 1 and 2 are equal ($Ya1b1 = Ya1c1 = Yc1c1 = Y_{11}$; $Ya2b2 = Ya2c2 = Yc2c2 = Y_{22}$; and $Ya1b2 = Ya1c2 = Ya2c1 = Yc1c2 = Y_{12} = Y_{21}$), model B is reduced to model A, with **Y**

$$\begin{bmatrix} 1 & 1 & 1 \\ 1 & Y_{11} & Y_{12} \\ 1 & Y_{21} & Y_{22} \end{bmatrix} \quad (2)$$

For both models, at a given total concentration of binding sites and ligands, the bound ligands are partitioned into three categories (isolated, end, or interior) by calculating the probability that a bound ligand has a certain neighbor using the conditional probabilities in Markov chain transition matrix **P**. When two different ligands are present, the concentrations of all end ligands with a different type of ligand as a neighbor are summed, as are the concentrations of all interior ligands with at least one neighbor of a different type.

Fitting Models to Data. *Photophysical Data.* The experimental pre-exponential factors (α values), from the data of titrations of AT-DNA with Δ- and Λ-Ru-phen in 5 mM phosphate buffer given by McKinley et al.,[21] were projected on the space spanned by the calculated probabilities *P* that a bound ligand belongs to one of the three categories (calculated as in Table 1) to obtain the least-square fit.

$$\alpha_{\text{short,calculated}} = c_{\text{isol}}P_{\text{isol}} + c_{\text{end}}P_{\text{end}} + c_{\text{int}}P_{\text{int}} \quad (3)$$

Table 1. Calculation of Category Probability

	isolated	end	interior
model A	P_{01}^2	$2P_{01}P_{11}$	P_{11}^2
model B	$\theta_d(\theta_d + 2\theta_a + \theta_c)^{-1}$	$2\theta_a(\theta_d + 2\theta_a + \theta_c)^{-1}$	$\theta_c(\theta_d + 2\theta_a + \theta_c)^{-1}$

ITC Data. The change in concentration upon addition of a ligand was calculated for the categories (three for Δ, three for Λ, and two for Δ−Λ pairs) as well as the change in concentration of ligand dimers and of externally bound ligands.[20,31] Ligand dimerization in solution was assumed not to be dependent on stereochemistry, whereas the external binding was assumed to be dependent on the chirality of the externally bound ligand but not on the chirality of the intercalated ligand. The entire ITC data set of one blank (buffer) and five ligand titrations (114 data points) was projected on the space of these concentration changes as 11 columns.

Global Fit. The sum of the residual norm of the ITC fit and of the fit to the α values was minimized by varying binding constants *K*, binding site coverage numbers *n*, cooperativity factors *y*, and dimerization constant K_m using the *fminsearch* function of MATLAB.

RESULTS

Isothermal Titration Calorimetry and Model Fitting. The raw ITC data with the enantiomers of Ru-phen and also racemic Ru-phen titrated into AT-DNA are shown in Figure 3. The ITC profiles in the left column show the ligand titrated into AT-DNA only. At the end of the titration, further injections with the same enantiomer (not shown) gave only very small constant heat values, indicating full saturation of the DNA. This is attributed to heat of dilution of the free ligands and is in accordance with our previous results.[17,20,31] Upon titration by switching to the opposite enantiomer, significant enthalpy changes are observed (Figure 3, right column), strongly indicating that both enantiomers are capable of displacing each other on the DNA strand.

We recently showed that the two categories of intrinsic binding and neighbor interaction, as calculated by model A (described in the Experimental Section), could give a good fit to the ITC curves for the pure enantiomers of Ru-phen.[31] In the Ru-bpy series, augmenting these categories with a single Δ−Λ neighbor interaction was found to produce a very good fit of model A to the competition curves.[20] For the ITC data set presented here, the fit of model A with two intrinsic binding (Δ and Λ) and three neighbor interaction (ΔΔ, ΛΛ,

DOI: 10.1021/acs.inorgchem.9b01298
Inorg. Chem. 2019, 58, 9452−9459

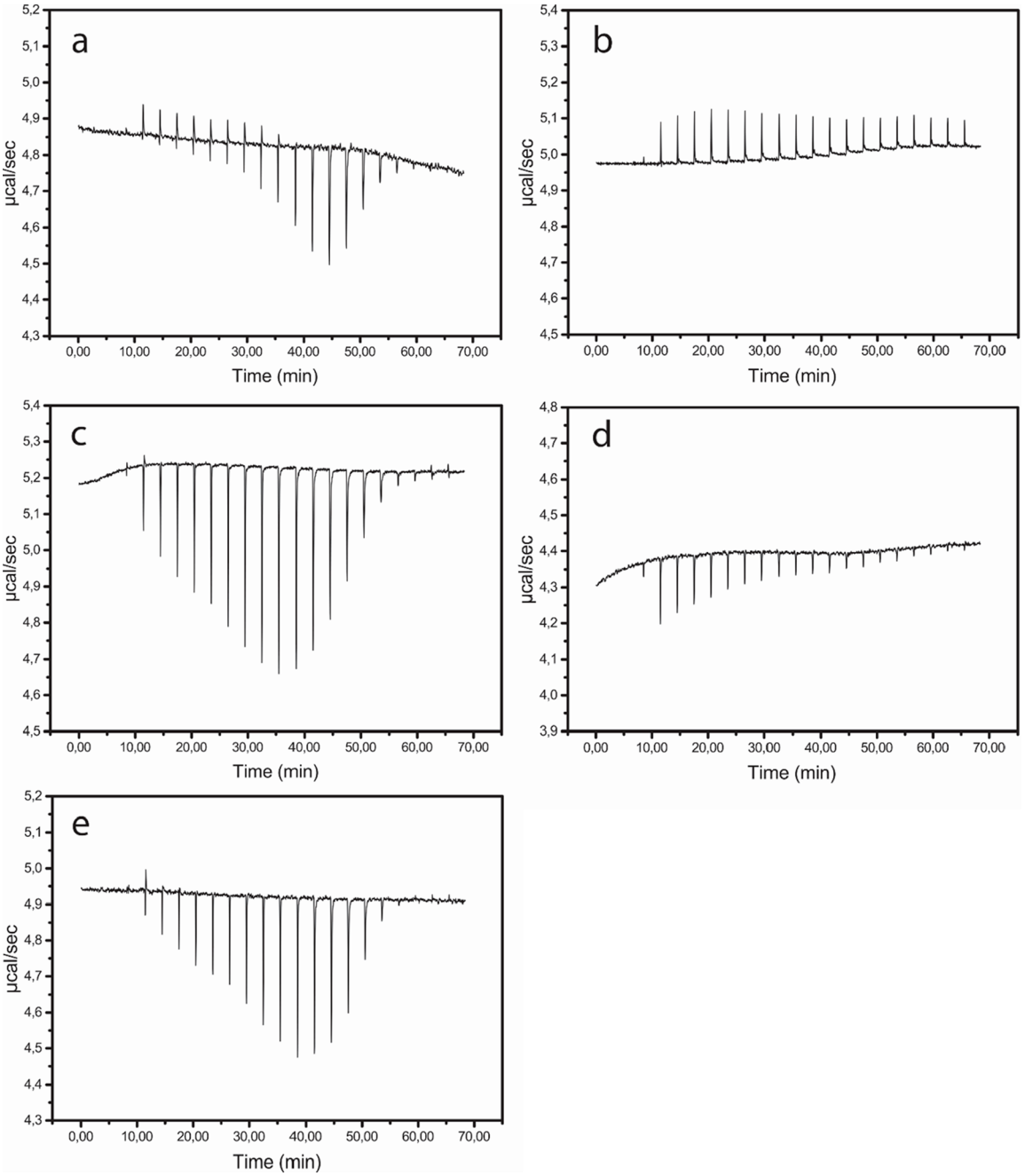

Figure 3. ITC raw data for binding of the Δ and Λ enantiomers of Ru-phen to AT-DNA alone [(a) Δ and (c) Λ] followed by a second titration of the opposite enantiomer to already ligand-saturated AT-DNA [(b) Δ into Λ-saturated DNA and (d) Λ into Δ-saturated DNA]. The bottom panel (e) shows racemic Ru-phen titrated into AT-DNA alone. All titrations were performed in an aqueous 150 mM NaCl buffer solution at 25 °C. A complex (~550 μM) was injected in 2 μL aliquots into the 206 μL cell containing the DNA (~408 μM nucleotides).

and ΔΛ) categories was not as good. A better fit to the ITC data was obtained when the neighbor interaction category was differentiated into an end and an interior contribution, as described above in the Experimental Section. Nevertheless, when calculating α values by assigning the long lifetime exclusively to the end category, model A failed completely to simultaneously fit the ITC and photophysical data. Similarly, model C, used in our previous global analysis of ITC and photophysical data for Ru-phen enantiomers, which assigned the long lifetime exclusively to the end category,[17] failed to produce an acceptable global fit.

The strict assignment of excited-state lifetimes to specific species defined by a binding model could be relaxed if it is assumed that every intercalated Ru complex could be in equilibrium between a long-lived and a short-lived species and that it is the corresponding equilibrium constant that is affected by the neighbors. Thus, assuming that the α values could be calculated according to eq 3 (see the Experimental Section) gave much better global fits.

For model A, the best fit was obtained by assuming equal binding to the alternating AT/AT and TA/TA steps. By contrast, for model B, the best fit was obtained when binding was assumed to occur exclusively at one of these steps.

DOI: 10.1021/acs.inorgchem.9b01298
Inorg. Chem. 2019, 58, 9452−9459

Moreover, binding site coverage parameter n could be set to be exactly 1 for both enantiomers without significantly increasing the residual norm. Figure 4 shows the best global fit to the

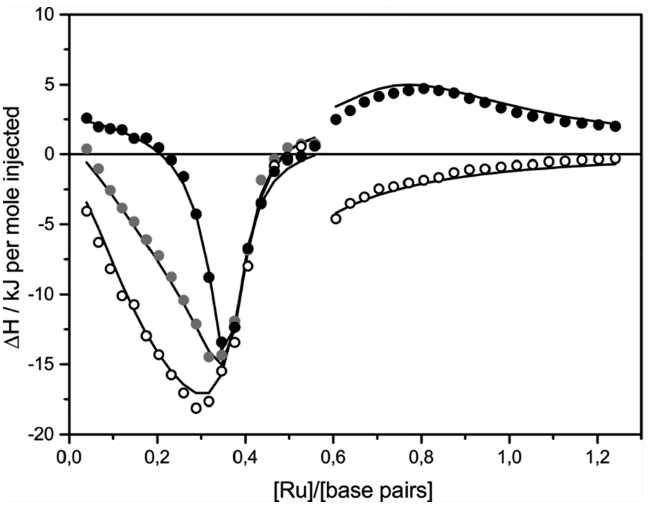

Figure 4. ITC profiles with fitted traces of model B for the titration of Δ- and Λ-Ru-phen to AT-DNA alone (left) followed by a second titration of the opposite enantiomer to already ligand-saturated AT-DNA (right). Also shown is the ITC profile for racemic Ru-phen titrated to AT-DNA alone. Circles (Δ, black; Λ, white; rac, gray) indicate the normalized integrated heat absorbed or evolved upon 19 sequential 2 μL injections of the complex (~550 μM) into the 206 μL cell containing the DNA (~408 μM nucleotides). All titrations were performed in a 150 mM NaCl aqueous solution at 25 °C.

integrated peaks of the raw data (Figure 3) using model B, which gave an nRMSD of 11.1% (Table 2) (nRMSD, normalized root-mean-square-deviation, the Euclidian norm of the residual divided by the Euclidian norm of the data).

Table 2. nRMSD Values for the Best Global Fit of ITC and Photophysical Data with Model A or Model B

	ITC	α
model A	14.3%	4.4%
model B	11.1%	2.5%

The best global fit obtained for model A is shown in Figure S1, which gave an nRMSD of 14.3% (Table 2). The ITC profiles with fitted traces for the averaged titrations of Δ- and Λ-Ru-phen to pure buffer are shown in Figure S2.

Table 3 compares the best global fit parameter values for model A and model B. Model A, with only one type of elementary unit, has only one cooperativity factor y, which showed a slight cooperativity in the nearest neighbor interactions of both Δ−Δ and Λ−Λ while Δ−Λ interactions were anticooperative. In model B, Δ showed modest cooperative interactions when bound to the DNA lattice as *a-b* (i.e., as an isolated dimer) but is essentially noncooperative as the isolated trimer *a-c-b* that very reluctantly expands to tetramers (e.g., *a-c-c-b*) due to the strong anticooperativity of the *c-c* interaction. In contrast, while the isolated trimer *a-c-b* is also noncooperative for Λ, the isolated dimer *a-b* is modestly anticooperative as is the *c-c* interaction. Interestingly, the values for the heterochiral interactions are closer to Λ than to Δ. The ΔH° values for the binding of the different categories from the global fitting of model A and model B are listed in Table 4,

Table 3. Binding Parameter Values from Global Fitting of Model A and Model B to ITC Data[a]

	K (×10^6)	n	y	y_{ab}	y_{ac}	y_{cc}
		Model A				
Δ	7.06	2.57	1.46			
Λ	2.09	2.31	1.08			
Δ−Λ			0.78			
dimer	2.0×10^{-4}					
		Model B				
Δ	13.7			2.70	1.12	0.07
Λ	3.71			0.45	0.93	0.25
Δ−Λ				0.70	1.26	0.19
dimer	2.9×10^{-4}					
	K (×10^6)	n_a/n_c		y_{ab}	y_{ac}	y_{cc}
		Model C				
Δ	1.1	2/1.8		56	6	0.01
Λ	0.2	2/1.8		9	9	0.05

[a]Included are also the parameters from the old model C (from ref 17).

Table 4. Enthalpy Parameter Values[a] from Global Fitting of Model A and Model B to ITC Data

	outer[b]	isolated	end	interior	end, mix	interior, mix	dimer
			Model A				
Δ	−1.0	−1.2	+1.4	−7.9	−11.0	−16.1	−14.2
Λ	+1.5	−5.0	−18.3	−14.9			
			Model B				
Δ	+0.4	−0.7	−0.6	−24.5	−7.4	−21.3	−24.1
Λ	+0.8	−4.4	−17.3	−14.3			

[a]ΔH° in kilojoules per mole. [b]Assuming K_{outer} = 100.

together with the enthalpy values for the outer binding mode to saturated DNA and the formation of a dimer in solution. Derived standard thermodynamic values for equilibrium parameters K and y_{ij} from the fit of model B are listed in Table 5, in which the cooperativity factor enthalpies were calculated by linear combination of the category enthalpies.

Figure 5 shows the best global fit for the experimental pre-exponential factors for the shorter lifetime α_s of Δ- and Λ-Ru-phen titrated to AT-DNA (data obtained from ref 21) using model B, which gave an nRMSD of 2.5% (Table 2). The best global fit obtained for model A is shown in Figure S3, which gave an nRMSD of 4.4% (Table 2). As the titration progresses, more and more binding sites on the DNA lattice become occupied by ligands; i.e., the DNA becomes saturated. Hence, the fraction of short excited-state lifetime, which is more associated with the isolated elementary unit *d*, decreases. For the Δ enantiomer, the ratio α_s is subsequently lower than for the Λ enantiomer, most likely caused by a higher number of *a-b* dimer conformations preferred by Δ. In addition, the slightly increased ratio α_s observed at the highest [Ru]/[base pairs] ratio for Δ is predicted to be caused by the reluctant formation of longer consecutive sequences like *a-c-c-b* in the sterically crowded DNA lattice.

Models A and B gave qualitatively similar results when fitted to the photophysical data, as shown in Table 6. It should be noted, however, that these data were obtained at a salt concentration (5 mM sodium phosphate buffer) much lower than that used in the ITC experiments and that it has been shown that the proportion of the long lifetime increases with

DOI: 10.1021/acs.inorgchem.9b01298
Inorg. Chem. 2019, 58, 9452−9459

Table 5. Standard Thermodynamic Quantities at 25 °C Derived from the Fit of Model B

	Δ				Λ			
	K	y_{ab}	y_{ac}	y_{cc}	K	y_{ab}	y_{ac}	y_{cc}
value	13.7×10^6	2.70	1.12	0.07	3.7×10^6	0.45	0.93	0.25
$\Delta G°$ (kJ mol^{-1})	−40.7	−2.5	−0.3	+6.6	−37.5	+2.0	+0.2	+3.4
$\Delta H°$ (kJ mol^{-1})	−0.7	+0.2	−11.8	−23.8	−4.4	−25.8	−17.8	−9.9
$\Delta S°$ (J mol^{-1} K^{-1})	+134	+8.9	−39	−102	+111	−93	−60	−45

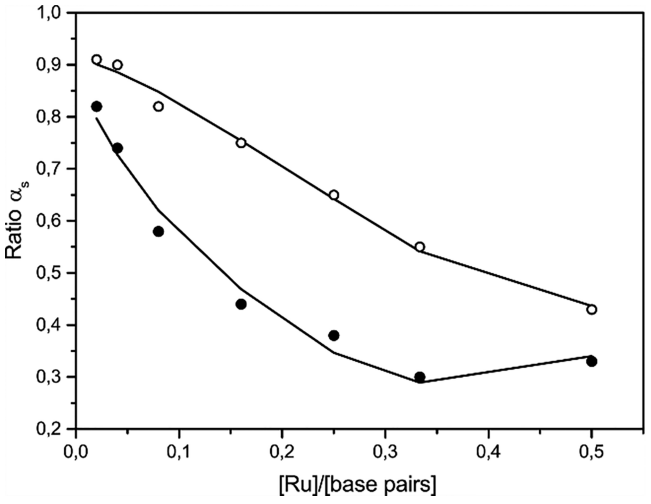

Figure 5. Fitted traces of model B to the α values for the short lifetime, with data taken from the titrations of AT-DNA with enantiopure Ru-phen (Δ, black circles; Λ, white circles) by McKinley et al.[21] All titrations were performed in 5 mM phosphate buffer at 25 °C.

Table 6. Coefficients c for the Best Fit to Experimental α_{short} Data

	isolated	end	interior
	Model A		
Δ	0.82	0	0.45
Λ	0.92	0.51	0.30
	Model B		
Δ	0.89	0.07	1.00
Λ	0.91	0.65	0.11

ionic strength;[22] thus, the results have to be interpreted with some caution. For Δ, the fit of model B assigns the short lifetime almost exclusively to isolated and interior ligands while the long lifetime is assigned to end ligands, in close parallel to our previous analysis that used a smaller set of α values obtained at the same high salt concentration as in ITC.[17] In contrast, for Λ the interior ligand is the dominating contributor to the long lifetime, with some end ligand contribution, as well.

DISCUSSION

Our previous global analysis of ITC and excited-state populations suggested that the two distinct lifetimes observed for each of the Ru-phen enantiomers bound to AT-DNA directly corresponded with two distinct binding geometries,[17] which were assigned to those observed by X-ray crystallography for the Λ enantiomer.[23] This immediate correspondence needs to be modified, if a binding model of the type investigated here can provide a satisfactory global fit to competitive ITC titration and excited-state population data. We suggest that instead of identification of each excited-state lifetime with a specific geometric arrangement in the intercalation pocket, each intercalated complex could be regarded as being in equilibrium between a short and a long lifetime state, and that it is this equilibrium that might be altered by the neighboring ligands. This suggestion further provides a plausible explanation for the observation that the short lifetime α value is found to decrease dramatically with temperature.[22] According to our previous model, because the value also decreases upon saturation of the DNA (see Figure 5) as the number of complex interactions increases, a large decrease in α_s at a fixed [Ru]/[base pairs] ratio upon a small increase in temperature implies a corresponding increase in the cooperativity factor, and hence, such an equilibrium must be endothermic. However, complex interaction equilibria are exothermic when monitored by ITC. Water hydrogen bonded to a phenazine nitrogen has been observed in an X-ray crystal structure.[24] Thus, we propose that a more likely endothermic process that could explain the endothermic decrease in the short lifetime population is the release of a slowly exchangeable water molecule hydrogen bonded to a phenazine nitrogen of the intercalated dppz chelate.

Even if we ignore the imperfect fit of model A to the competitive ITC titrations (see Figure S1), model B presents two advantages over model A in the physical interpretation of the model parameters.

(1) A specificity for the TA/TA steps of the DNA polymer is inherent in the model, consistent with recent X-ray crystallographic data showing the dppz ligand of Λ-Ru(phen)$_2$dppz^{2+} intercalates at the TA/TA step but not at the AT/AT step of a DNA duplex.[23]

(2) Binding site coverage number n can be set to unity for all bound ligands regardless of their environment, instead of being a freely adjustable non-integer parameter with different values for Δ and Λ. Thus, in model B, all diastereomeric variation in binding affinity parameters is contained in the values of K and y_{ij}.

Although model C, employed in our previous global analysis, gave the same n values for Δ- and Λ-Ru-phen (2.0 for elementary units a and b and 1.8 for c), it gave a large span (0.01−56) in the value of cooperativity parameter y, and it was not able to fit the competitive ITC data. With model B, the span is much smaller (0.07−2.7), which facilitates a rationalization of the diastereomeric differences in structural terms. Our data support the conjecture, originally made by Barton et al. for Ru(phen)$_3^{2+}$ more than 30 years ago,[18] that a higher intrinsic binding constant K for Δ enantiomers of trigonal metallo-intercalators is to be expected due to their better fit to the groove(s) of a right-handed double helix. Furthermore, the values of the cooperativity parameters suggest that a general steric crowding resists full lattice saturation ($y_{cc} < 1$ for all combinations) but that this crowding is modulated by diastereomeric differences in the attractive and repulsive intermolecular contacts.

DOI: 10.1021/acs.inorgchem.9b01298
Inorg. Chem. 2019, 58, 9452−9459

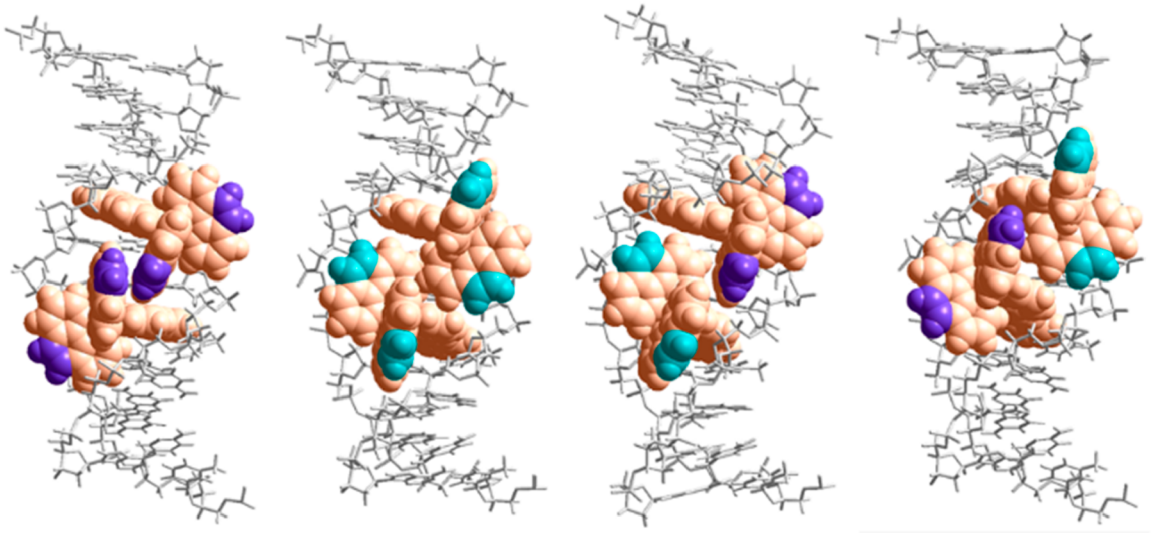

Figure 6. Schematic illustration of the proposed nearest neighbor interaction geometries for the Δ and Λ enantiomers of $Ru(phen)_2dppz^{2+}$ when intercalated to DNA via the minor groove. The 5,6-carbons on the phen moieties are highlighted (Δ, purple; Λ, cyan). The models were constructed by manual docking and subsequent energy minimization in a vacuum, using the Amber 2 force field in the HyperChem 8.0 software package (HyperCube, Inc.).

As seen from the molecular models in Figure 6, the phenanthroline B rings can make close contact only for the homochiral ΔΔ pairs, which is consistent with the heterochiral *y* values being more similar to those of ΛΛ than to those of ΔΔ. As previously suggested, the added bulk and hydrophobicity of the fused benzene ring of phenanthroline appear to have very little influence on the cooperativity parameters for Λ, which would explain the similarity in the ITC and luminescence data for the Λ enantiomers of Ru-phen and Ru-bpy and the dissimilarity in the data for the Δ enantiomers.[17]

The values of the *y* parameters can be expected to be a product of both attractive and repulsive factors, of which we expect the four most important to be (1) a repulsive factor from the electrostatic repulsion of neighboring positive cations, (2) a repulsive factor due to intercomplex steric clashes, (3) an attractive factor due to hydrophobic/stacking interactions, primarily for Δ, and (4) an attractive factor from binding to a groove already widened by the first bound complex, primarily for Λ.

Because the y_{ac} parameter is close to unity for both homo- and heterochiral combinations, it appears that in all triplets *a-c-b*, the repulsive and attractive contributions seem to balance. The Δ enantiomer forms cooperative *a-b* pairs but very uncooperative *a-c-c-b* quartets, suggesting that a weak hydrophobic attractive type 3 factor is gradually overcome by a steric repulsive type 2 factor. By contrast, for the Λ enantiomer, the steric repulsive type 2 factor seem less prominent and is balanced by an attractive type 4 factor, slightly favoring isolated complexes *d* over *a-c-b* triplets. The pronounced diastereomeric differences in the binding enthalpy and entropy values in Table 5 for the binding equilibria are very likely to reflect the differences in the contributing factors discussed above; however, we believe that it would be too speculative to attempt to resolve the contribution of each factor.

CONCLUSIONS

Even though our previous model for the ligand−DNA interactions of $Ru(phen)_2dppz^{2+}$ gave a satisfactory global fit for both calorimetric and photophysical experimental data by directly connecting the two distinct excited-state emission decays characteristic of this complex with two distinct binding geometries, it could not fit the competitive calorimetric titrations and would not properly explain the observed salt concentration and temperature dependence of the lifetime fractions without an extreme salt or temperature dependence of the equilibrium parameters. Here, we propose a different interpretation, where all intercalated complexes are instead regarded to be in equilibrium between a short and a long lifetime state, which we suggest is due to the presence or absence of a slowly exchanged water molecule hydrogen bonding to a phenazine nitrogen, and this equilibrium is affected by interactions from neighboring bound ligands. We suggest that the steric crowding of the bulky ancillary ligands causes a general resistance of forming longer sequential chains of bound complexes, which is supported by the small value of the cooperativity parameter between internal complexes. This is further consistent with the diastereomeric differences in intermolecular contacts suggested by molecular models. Although the model is limited to explaining the complex behavior of ITC and time-resolved luminescence data for simple repeating DNA sequences, its physical concepts provide a basis for a rough understanding of the interaction of Ru complexes and other bulky DNA intercalators with genomic DNA, as well.

ASSOCIATED CONTENT

Supporting Information

The Supporting Information is available free of charge on the ACS Publications website at DOI: 10.1021/acs.inorgchem.9b01298.

ITC profiles with fitted traces for model A for the competitive titration of enantiopure and racemic Ru-phen to AT-DNA, ITC profiles with fitted traces of model A and model B for the averaged titrations of enantiopure Ru-phen to pure buffer, and fitted traces of model A to the α values for the short lifetime of enantiopure Ru-phen (PDF)

DOI: 10.1021/acs.inorgchem.9b01298
Inorg. Chem. 2019, 58, 9452−9459

AUTHOR INFORMATION

Corresponding Author

*E-mail: lincoln@chalmers.se.

ORCID

Anna K. F. Mårtensson: 0000-0002-8786-4965

Maria Abrahamsson: 0000-0002-6931-1128

Notes

The authors declare no competing financial interest.

ACKNOWLEDGMENTS

The authors thank Dr. Johanna Andersson for her contributing work in relation to this study. The authors gratefully acknowledge the Swedish Research Council (Vetenskapsrådet) (2016-05421) and the Chalmers Area of Advance Nano for funding this project. The authors also thank COST Action CM1105 and the European MicroCal meetings for providing forums for stimulating discussions.

REFERENCES

(1) Friedman, A. E.; Chambron, J. C.; Sauvage, J. P.; Turro, N. J.; Barton, J. K. Molecular light switch for DNA − $Ru(bpy)_2$ $dppz^{2+}$. *J. Am. Chem. Soc.* **1990**, *112*, 4960−4962.

(2) Jenkins, Y.; Friedman, A. E.; Turro, N. J.; Barton, J. K. Characterization of dipyridophenazine complexes of ruthenium(II): the light switch effect as a function of nucleic acid sequence and conformation. *Biochemistry* **1992**, *31*, 10809−10816.

(3) Hartshorn, R. M.; Barton, J. K. Novel dipyridophenazine complexes of ruthenium(II) − exploring luminescent reporters of DNA. *J. Am. Chem. Soc.* **1992**, *114*, 5919−5925.

(4) Gill, M. R.; Thomas, J. A. Ruthenium(II) polypyridyl complexes and DNA − from structural probes to cellular imaging and therapeutics. *Chem. Soc. Rev.* **2012**, *41*, 3179−3192.

(5) Erkkila, K. E.; Odom, D. T.; Barton, J. K. Recognition and reaction of metallointercalators with DNA. *Chem. Rev.* **1999**, *99*, 2777−2795.

(6) Coates, C. G.; Olofsson, J.; Coletti, M.; McGarvey, J. J.; Önfelt, B.; Lincoln, P.; Nordén, B.; Tuite, E.; Matousek, P.; Parker, A. W. Picosecond time-resolved resonance Raman probing of the light-switch states of $Ru(phen)_2$ $dppz^{2+}$. *J. Phys. Chem. B* **2001**, *105*, 12653−12664.

(7) Olson, E. J. C.; Hu, D.; Hormann, A.; Jonkman, A. M.; Arkin, M. R.; Stemp, E. D. A.; Barton, J. K.; Barbara, P. F. First observation of the key intermediate in the "light-switch" mechanism of $Ru(phen)_2$ $dppz^{2+}$. *J. Am. Chem. Soc.* **1997**, *119*, 11458−11467.

(8) Önfelt, B.; Lincoln, P.; Nordén, B.; Baskin, J. S.; Zewail, A. H. Femtosecond linear dichroism of DNA-intercalating chromophores: Solvation and charge separation dynamics of $Ru(phen)_2$ $dppz^{2+}$ systems. *Proc. Natl. Acad. Sci. U. S. A.* **2000**, *97*, 5708−5713.

(9) Olofsson, J.; Önfelt, B.; Lincoln, P.; Nordén, B.; Matousek, P.; Parker, A. W.; Tuite, E. M. Picosecond Kerr-gated time-resolved resonance Raman spectroscopy of the $Ru(phen)_2$ $dppz^{2+}$ interaction with DNA. *J. Inorg. Biochem.* **2002**, *91*, 286−297.

(10) McKinley, A.; Lincoln, P.; Tuite, E. M. Environmental effects on the photophysics of transition metal complexes with dipyrido 2,3-a:3′,2′-c phenazine (dppz) and related ligands. *Coord. Chem. Rev.* **2011**, *255*, 2676−2692.

(11) Olofsson, J.; Önfelt, B.; Lincoln, P. Three-state light switch of $Ru(phen)_2$ $dppz^{2+}$: Distinct excited-state species with two, one, or no hydrogen bonds from solvent. *J. Phys. Chem. A* **2004**, *108*, 4391−4398.

(12) Westerlund, F.; Pierard, F.; Eng, M. P.; Nordén, B.; Lincoln, P. Enantioselective luminescence quenching of DNA light-switch $Ru(phen)_2$ $dppz^{2+}$ by electron transfer to structural homologue $Ru(phendione)_2$ $dppz^{2+}$. *J. Phys. Chem. B* **2005**, *109*, 17327−17332.

(13) Olofsson, J.; Wilhelmsson, L. M.; Lincoln, P. Effects of methyl substitution on radiative and solvent quenching rate constants of $Ru(phen)_2$ $dppz^{2+}$ in polyol solvents and bound to DNA. *J. Am. Chem. Soc.* **2004**, *126*, 15458−15465.

(14) Hiort, C.; Lincoln, P.; Nordén, B. DNA binding of Δ- and Λ-$[Ru(phen)_2DPPZ]^{2+}$. *J. Am. Chem. Soc.* **1993**, *115*, 3448−3454.

(15) Haq, I.; Lincoln, P.; Suh, D. C.; Nordén, B.; Chowdhry, B. Z.; Chaires, J. B. Interaction of Δ- and Λ-$[Ru(phen)_2DPPZ]^{2+}$ with DNA − a calorimetric and equilibrium binding study. *J. Am. Chem. Soc.* **1995**, *117*, 4788−4796.

(16) Lincoln, P.; Broo, A.; Nordén, B. Diastereomeric DNA-binding geometries of intercalated ruthenium(II) trischelates probed by linear dichroism: $[Ru(phen)_2DPPZ]^{2+}$ and $[Ru(phen)_2BDPPZ]^{2+}$. *J. Am. Chem. Soc.* **1996**, *118*, 2644−2653.

(17) Andersson, J.; Fornander, L. H.; Abrahamsson, M.; Tuite, E.; Nordell, P.; Lincoln, P. Lifetime heterogeneity of DNA-bound dppz complexes originates from distinct intercalation geometries determined by complex-complex interactions. *Inorg. Chem.* **2013**, *52*, 1151−1159.

(18) Barton, J. K.; Danishefsky, A. T.; Goldberg, J. M. Tris-(phenanthroline)ruthenium(II) − stereoselectivity in binding to DNA. *J. Am. Chem. Soc.* **1984**, *106*, 2172−2176.

(19) Lincoln, P.; Nordén, B. Binuclear ruthenium(II) phenanthroline compounds with extreme binding affinity for DNA. *Chem. Commun.* **1996**, 2145−2146.

(20) Mårtensson, A. K. F.; Lincoln, P. Competitive DNA binding of $Ru(bpy)_2$ $dppz^{2+}$ enantiomers studied with isothermal titration calorimetry (ITC) using a direct and general binding isotherm algorithm. *Phys. Chem. Chem. Phys.* **2018**, *20*, 7920−7930.

(21) McKinley, A. W.; Andersson, J.; Lincoln, P.; Tuite, E. M. DNA sequence and ancillary ligand modulate the biexponential emission decay of intercalated $Ru(L)_2$ $dppz^{2+}$ enantiomers. *Chem. - Eur. J.* **2012**, *18*, 15142−15150.

(22) McKinley, A. W.; Lincoln, P.; Tuite, E. M. Sensitivity of $Ru(phen)_2$ $dppz^{2+}$ light switch emission to ionic strength, temperature, and DNA sequence and conformation. *Dalton Trans.* **2013**, *42*, 4081−4090.

(23) Niyazi, H.; Hall, J. P.; O'Sullivan, K.; Winter, G.; Sorensen, T.; Kelly, J. M.; Cardin, C. J. Crystal structures of λ-$[Ru(phen)_2$ $dppz]^{2+}$ with oligonucleotides containing TA/TA and AT/AT steps show two intercalation modes. *Nat. Chem.* **2012**, *4*, 621−628.

(24) Hall, J. P.; Cook, D.; Morte, S. R.; McIntyre, P.; Buchner, K.; Beer, H.; Cardin, D. J.; Brazier, J. A.; Winter, G.; Kelly, J. M.; Cardin, C. J. X-ray crystal structure of rac-$[Ru(phen)_2$ $dppz]^{2+}$ with $d(ATGCAT)_2$ shows enantiomer orientations and water ordering. *J. Am. Chem. Soc.* **2013**, *135*, 12652−12659.

(25) Mårtensson, A. K. F.; Lincoln, P. Binding of Ru(terpyridine)-(pyridine)dipyridophenazine to DNA studied with polarized spectroscopy and calorimetry. *Dalton Trans.* **2015**, *44*, 3604−3613.

(26) McGhee, J. D.; von Hippel, P. H. Theoretical aspects of DNA-protein interactions − cooperative and non-cooperative binding of large ligands to a one-dimensional homogenous lattice. *J. Mol. Biol.* **1974**, *86*, 469−489.

(27) Lincoln, P. A generalized McGhee-von Hippel method for the cooperative binding of different competing ligands to an infinite one-dimensional lattice. *Chem. Phys. Lett.* **1998**, *288*, 647−656.

(28) Jelesarov, I.; Bosshard, H. R. Isothermal titration calorimetry and differential scanning calorimetry as complementary tools to investigate the energetics of biomolecular recognition. *J. Mol. Recognit.* **1999**, *12*, 3−18.

(29) Ladbury, J. E.; Chowdhry, B. Z. Sensing the heat: The application of isothermal titration calorimetry to thermodynamic studies of biomolecular interactions. *Chem. Biol.* **1996**, *3*, 791−801.

(30) Wiseman, T.; Williston, S.; Brandts, J. F.; Lin, L. N. Rapid measurement of binding constants and heats of binding using a new titration calorimeter. *Anal. Biochem.* **1989**, *179*, 131−137.

(31) Mårtensson, A. K. F.; Lincoln, P. Effects of methyl substitution on DNA binding enthalpies of enantiopure $Ru(phenanthroline)_2$ $dipyridophenazine^{2+}$ complexes. *Phys. Chem. Chem. Phys.* **2018**, *20*, 11336−11341.

DOI: 10.1021/acs.inorgchem.9b01298
Inorg. Chem. 2019, 58, 9452−9459